OL | Organic Letters

pubs.acs.org/OrgLett Letter

Synthesis and Structural Characterization of 2′-Deoxy-2′-fluoro-L-uridine Nucleic Acids

Yuliya Dantsu, Ying Zhang, and Wen Zhang*

Cite This: *Org. Lett.* 2021, 23, 5007−5011 Read Online

ACCESS | Metrics & More | Article Recommendations | Supporting Information

ABSTRACT: Despite the development of artificial L-RNA/DNA as therapeutic molecules, the in-depth investigation on their chemical modifications is still limited. Here, we synthesize a chemically derivatized 2′-deoxy-2′-fluoro-L-uridine building block and incorporate it into oligonucleotides. Our thermo-denaturization and enzymatic digestion experiments reveal their superior stability. Furthermore, one crystal structure of L-type fluoro-DNA is determined to characterize its handedness. Our results reveal the increase of L-helix stability by fluoro-modification and provide the foundation for its future functional application.

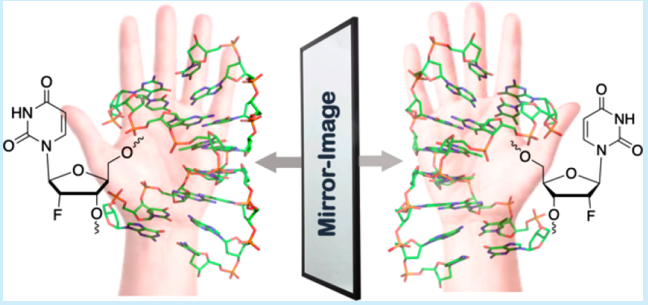

Nucleic acid ligands are able to fold into three-dimensional structures with high affinities for a variety of molecular targets, from small ions to entire organisms.[1] The development of Systematic Evolution of Ligands by EXponential enrichment (SELEX) has enabled the isolation of functional oligonucleotides from combinatorial libraries through *in vitro* selection methods.[2] As a result of feasibility with DNA and RNA libraries, aptamers are becoming attractive advanced tools for use in disease diagnostic and therapeutic application. Nevertheless, one of the seemingly intractable challenges of aptamer drugs is their short half-life *in vivo*. For instance, the ubiquitous nucleases in human body can cause the rapid degradation of natural RNA/DNA molecules, which limits their practicability in pharmaceutical application.[3] To date, tremendous efforts have been devoted targeting nucleic acid structures to engender the stable candidates in biological fluids.[4] Some nuclease-resistant oligonucleotides have been successfully isolated by selection from the modified libraries or post-modification of aptamers.

One approach has been adapted to potently optimize nucleic acid therapies by utilizing the DNA/RNA molecules with radically different chirality from their native counterparts.[5] The principle is bolstered by the observation that the L-type enantio-nucleic acid ligands display the identical physical, chemical, and structural properties in terms of solubility and structural stability as D-nucleic acids. Furthermore, due to the chiral inversion, the L-nucleic acids are unrecognizable by any nucleases in plasma, resulting in the greatly extended half-life *in vivo*.[6] There have been various applications of L-DNA/RNA in nucleic acid therapeutics and diagnostics, including the L-aptamers with distinct three-dimensional structures and excellent binding affinities to molecular targets,[7] the microarray platform involving design of probes with L-DNA sequence stems,[8] the design of a catalytic L-DNA hairpin assembly as the stable signal amplifier,[9] the design of antisense L-/D-oligodeoxynucleotide chimeras,[10] and the L-DNA containing nanotechnology for material science and drug delivery.[11]

Despite the enhancement in stability, it is still critical to further explore the chemical optimization of L-nucleic acids in order to expand their functionalities. It is evident that chemical modifications on D-nucleic acid aptamer can considerably improve thermal and structural stabilities (in certain regions) and offer additional physicochemical diversity.[12] However, compared to the D-aptamer, much less chemical diversity has been pioneered in L-aptamer SELEX. Indeed, the inadequacy of chemically modified L-nucleic acid is a bottleneck that restricts the success rate of selection. To date, the reported example includes the utilization of L-5-aminoallyl-uridine, which has the chemical moiety at the 5-position of uridine that plays a critical role for molecular interaction.[13] Besides, the fluoro-modification has also been successfully introduced into the 2′-position of L-deoxyribose of pyrimidine,[14] but there is a lack of detailed thermodynamic and structural characterizations. On the other hand, the native D-type 2′-deoxy-2′-fluoro-ribonucleotides have wide beneficial applications, because of not only the nuclease resistance *in vivo* but also the enthalpy-based stability enhancement as a result of 2′-F induced strengthening of H-bonding and stacking interactions.[15] The electron-withdrawing fluoro-derivatization at the 2′-position of L-deoxyribose should also restrain the sugar

Received: May 1, 2021
Published: June 18, 2021

predominantly to L-type C3′-*endo* conformation, thereby enhancing the helical structural and thermal stability of L-duplex. Herein, we employed the chemical synthesis of L-type 2′-deoxy-2′-F-uridine building block and its oligonucleotides, and further carried out comprehensive studies to reveal more insights into structural and functional properties.

The idea of incorporation of a relatively small fluorine atom into a carbohydrate moiety of nucleosides relies on its ability to mimic the features of the hydroxyl group (similar van der Waals radii and polarity) and act as an acceptor by creating hydrogen bonds. Investigations of fluoro-modified nucleotides revealed better binding affinity to targets and nucleases resistance. For instance, the replacement of 2′- and 3′-hydroxyl groups by fluorine lead to nucleosides with potential antiviral effect, while the presence of two geminal fluorine atoms at C-2′ position resulted in chemotherapy medication Gemcitabine.[16] In this work, we attempted to chemically modify the nucleic acid molecules by both converting the handedness to L-type and introducing an additional 2′-F-substituent to the backbone.

The organic synthesis of the target phosphoramidite started from the commercially available L-type 2,2′-anhydrouridine **1**, followed by protecting the 3′ and 5′ positions by a tetrahydropyranyl group (Scheme 1), as described earlier.[14]

Scheme 1. Synthesis of L-Type 2′-Deoxy-2′-fluorouridine Phosphoramidite (6) and Oligonucleotide (7)

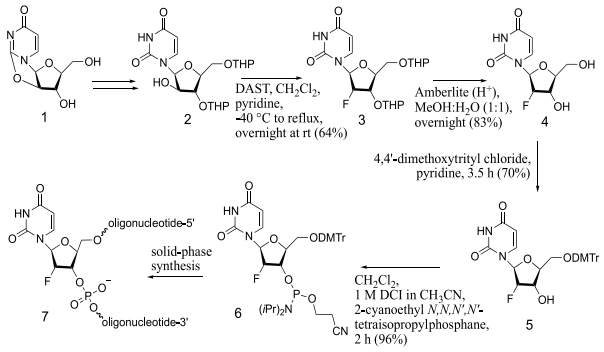

Subsequent hydrolysis reaction and fluorination with DAST reagent gave rise to the compound **3** in 64% overall yield. The deprotection of 2′-deoxy-2′-fluoro-3′,5′-di-*O*-tetrahydropyranyl-*β*-L-uridine could be realized by treatment with either *p*-TsOH in MeOH at room temperature for 3 h[17] or with Amberlite (H^+) in aqueous methanol overnight.[18] However, we found that the first method generated traces of *p*-toluenesulfonic acid that might catalyze detritylation reaction and reduce the yield of the target compound. In this work, we chose to deprotect the compound **3** under Amberlite (H^+) resin in aqueous methanol in 83% overall yield. The tritylation reaction was carried out by treating substance **4** with 4,4′-dimethoxytrityl chloride in dry pyridine. The key phosphoramidite **6** could be synthesized by applying two commonly used phosphitylation reagents, such as 2-cyanoethyl *N,N*-diisopropylchlorophosphoramidite (PCl) and 2-cyanoethyl *N,N,N′,N′*-tetraisopropylphosphorodiamidite (PN2). However, by treating substance **5** with PCl, the phosphitylation reaction could only be successfully accomplished for a small scale (up to 200 mg). The target compound **6** was finally synthesized in high yield in a larger scale in the presence of PN2 and activating reagent such as 4,5-dicyanoimidazole (DCI). Furthermore, DCI, as an activator, also promotes a coupling step in the solid-phase synthesis of oligonucleotides.

Compared to DNA, the fluoro-functionality at the 2′-position of our synthetic nucleoside phosphoramidite may cause the steric hindrance effect during the coupling step of solid-phase synthesis. Consequently, an extended coupling time of 180 s was applied in each L-U_F coupling. To avoid the unintended fluoride degradation, we chose the concentrated ammonium hydroxide solution, instead of AMA solution, for the nucleobase deprotection. The modified L-U_F monomer was successfully incorporated into the oligonucleotides at quantitative yield.

In the practical application, some chemical modifications have been introduced to the aptamers in order to reduce the conformational flexibility and increase the thermal stability.[19] In order to explore the potential stabilizing effect caused by the 2′-F moiety, we performed the thermal denaturation studies to measure the melting temperatures of various L-type duplexes. The Sybr green I fluorescent dye was used in T_m measurement, which could nonspecifically bind to double-stranded, not single-stranded, nucleic acid to induce fluorescent signal.[20]

We first decided to examine the effect of L-2′-F derivatization in L-DNA duplexes. The melting temperature of L-DNA duplex 5′-ATGGTGCTC-3′/5′-GAGCACCAT-3′ (entry a, Table 1) was measured to be 49.7 °C. It is worth

Table 1. MS Analysis and T_m Measurement of Synthetic L-Oligonucleotides (n.d. = Not Determined)

entry	sequences	isotopic mass *m*/*z* measured (calcd)	duplex T_m (°C)
a	L-5′-dATGGTGCTC-3′	$[M-2H]^{2-}$: 1363.3 (1363.2)	49.7 ± 0.4
b	L-5′-dATGGdUGCTC-3′	$[M-2H]^{2-}$: 1356.7 (1356.7)	43.2 ± 0.2
c	L-5′-dATGGdUGCdUC-3′	$[M-2H]^{2-}$: 1349.7 (1349.7)	41.8 ± 0.3
d	L-5′-dATGGU_FGCTC-3′	$[M-2H]^{2-}$:1365.2 (1365.2)	44.9 ± 0.5
e	L-5′-dATGGU_FGCU_FC-3′	$[M-2H]^{2-}$: 1367.2 (1367.2)	43.7 ± 0.6
f	L-5′-rGCAAAUUUGC-3′	$[M-2H]^{2-}$: 1570.8 (1570.7)	48.5 ± 0.5
g	L-5′-rGCAAAUUU$_F$GC-3′	$[M-2H]^{2-}$: 1571.7 (1571.7)	49.3 ± 0.2
h	L-5′-rGCAAAUU_FU$_F$GC-3′	$[M-3H]^{3-}$: 1047.9 (1048.1)	49.9 ± 0.7
i	L-5′-dGCAAATTTGC-3′	$[M-3H]^{3-}$: 1007.3 (1007.5)	52.4 ± 0.3
j	L-5′-dGTGTACAC-3′	$[M-2H]^{2-}$: 1202.8 (1203.2)	n.d.
k	L-5′-dGU$_F$GTACAC-3′	$[M-2H]^{2-}$: 1205.1 (1205.1)	n.d.

noting that our synthetic 2′-F-dU monomer is lacking a methyl group at the 5-position compared to L-thymidine, and it is known that the C5 group can help to stabilize the DNA helical conformation.[21] Therefore, to have the comprehensive comparison, we synthesized two additional L-DNA duplexes, which contained L-deoxyuridine residues to replace L-thymidines at the corresponding positions (entries b and c). When one L-T was substituted by L-dU, the melting temperature was dropped to 43.2 °C; moreover, when two L-dUs were present at the same duplex, the T_m was further decreased to 41.8 °C. This result fully revealed the importance of 5-methyl in the thymidine base when stabilizing the L-DNA

https://doi.org/10.1021/acs.orglett.1c01498
Org. Lett. 2021, 23, 5007−5011

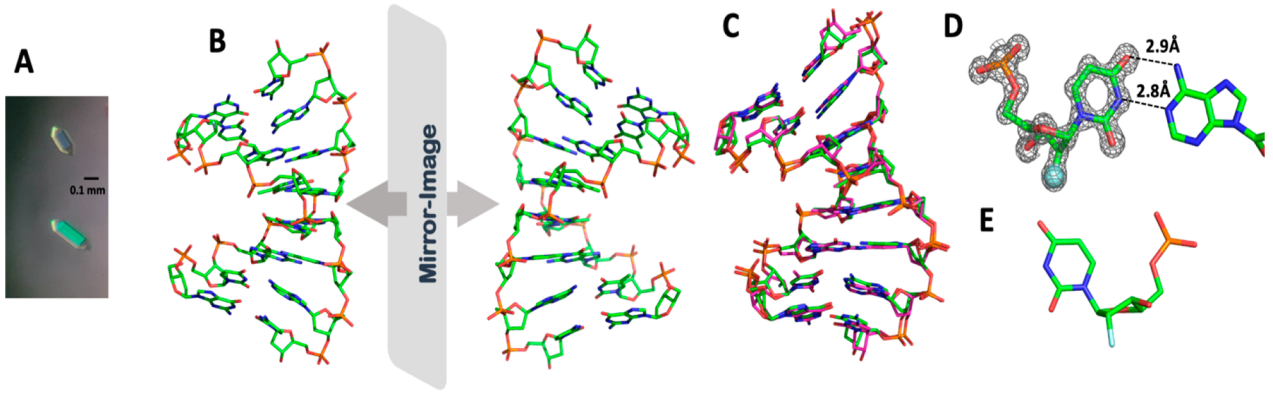

Figure 1. Crystal structures of fluoro-modified L-DNA. A: Crystals of fluoro-modified L-DNA octamer. B: Stereoview of fluoro-L-DNA 8-mer (left, resolution = 1.03 Å) and its mirror-image D-DNA 8-mer (right, PDB 1d79). C: Superimposed structures of fluoro-modified L-DNA (green) and the mirror reflection of D-DNA structure (purple). D: Modified L-U_F:L-A Watson−Crick base pair. Gray mesh indicates the corresponding $2F_o-F_c$ maps contoured at 1.0 σ. E: 2′-deoxy-2′-F-L-uridine in the 3′-*endo*-conformation.

double helix. When we replaced one L-deoxyuridine by L-2′-F-2′-deoxyuridine (entry d), the T_m was enhanced by 1.7 °C, to 44.9 °C. Besides, when 2 fluoro-modified residues were introduced to replace L-deoxyuridines (entry e), the T_m could be improved by 1.9 °C, to 43.7 °C. These melting studies lend evidence that bringing in fluoro-modification to the 2′-position could give rise to a more stable L-DNA duplex, although the 2′-*exo*-F conformationally disagrees with the 2′-*endo* conformation in canonical L-deoxyribose. Even so, the 5-methyl group of L-thymidine has a more consequential impact on the stability of L-DNA.

On the other hand, after incorporating the 2′-F into the L-RNA backbone, we observed slightly enhanced thermal stability. The self-complementary L-RNA 5′-GCAAAUUUGC-3′ (entry f) displayed a T_m of 48.5 °C, while the introduction of 2′-F moieties increased the T_m by 0.8 and 1.4 °C, respectively (entries g and h). Considering that the modifications existed pairwise in the self-complementary duplexes, this finding indicates that the small fluorine atoms caused a mild T_m increase (∼0.4 °C per modification), probably due to the conformational rigidity to the L-type A-form. Our results are consistent with the possibility that the 2′-F group could, due to enthalpy, stabilize the native RNA structures.[22] When the entire oligonucleotide was converted to L-DNA with the same sequence (entry i), the melting temperature was measured to be 52.4 °C, much higher than the duplexes containing the same sequence but all the ribo-residues. We expect that this striking boost is engendered by the three consecutive L-thymidines in the oligo, which totally leads to six 5-methyl groups in the double helix. For comparison, we also measured the thermostability of a set of 2′-F modified D-RNA (Table S1). The conclusion is similar to our observation regarding L-oligonucleotides, that one fluoro-modification could enhance the T_m by ∼0.4 °C. Interestingly, the overall T_m values of D-RNAs are lower than the mirror-image L-counterparts, and the reason might be the asymmetrical nature of the intercalating SYBR green dye, which causes the different binding patterns between D- and L- forms.

Susceptibility to nuclease degradation is a significant limitation to the design and utilization of aptamer drugs *in vivo*. Here we examined the stability of 2′-fluoro-modified L-oligonucleotides in human serum solution. We used four different RNA oligonucleotides, which shared the same sequence, but possessed different chirality and modification (oligo f: L-5′-rGCAAAUUUGC-3′, oligo g: L-5′-rGCAAAUUU_FGC-3′, oligo f′: D-5′-rGCAAAUUUGC-3′, oligo g′: D-5′-rGCAAAUUU_FGC-3′). The RNA samples were incubated with 0.5% human serum at 37 °C, followed by denaturing PAGE analysis (Figures S22 and S23). It was observed that the native oligo f′ was completely digested within 1 h without any intact strand detectable. Even after modification with one 2′-F-Uridine residue, the D-RNA g′ only displayed slightly improved stability and could not survive in serum longer than 2 h. In contrast, the L-RNA f and g, either wild-type or modified by a fluoride group, remained intact after 24 h of incubation with serum, without any fragmental cleavage product observed. It reveals that both fluoro-modified and nonmodified L- nucleic acids have dramatically enhanced biological stability in physiological environments, which is much stronger than the traditional 2′-F modification in gene therapy.

We then performed the circular dichroism studies to characterize the chiralities of our synthetic oligonucleotides. Two sets of fluoro-modified duplexes, including both L- and D-formed oligonucleotides (DNA d and d′ and RNA g and g′), were tested. The corresponding spectra are shown in Figure S24. The data revealed that the D-form 2′-F-modified DNA molecule adopted a B-form-like conformation, which provided a conservative CD spectrum with the following amplitude bands: a high positive band around 278 nm and a short negative one around 238 nm. In contrast, its mirror-image counterpart showed the chiral inversion (high negative around 278 nm and short positive around 238 nm, Figure S24A). For the native 2′-F-modified RNA, the CD spectrum was characterized as the A-form-like duplex, by a high positive band at 266 nm, a negative one at 236 nm, and a short positive band at 224 nm. Its chiral inversion was displayed when the modified L-RNA oligonucleotide was assessed (Figure S24B). The CD characterization illustrates the synthetic fluoro-modified L-DNA and L-RNA adopt the mirror-image helical conformations of their D-form fluoro-counterparts.

In order to investigate the structural features of the 2′-fluoro moiety on the L-ribose backbone, we then attempted to crystallize a self-complementary L-DNA 8-mer, 5′-GU$_F$GTACAC-3′, by screening 384 commercial conditions at 18 °C. Subsequently, we performed optimization of promising crystal growth, which included amplifying the crystallization drop and adjusting the concentrations of

https://doi.org/10.1021/acs.orglett.1c01498
Org. Lett. 2021, 23, 5007−5011

precipitant and DNA. The best crystal obtained was a rod-shaped specimen (Figure 1A) grown under 0.08 M NaCl, 0.02 M $MgCl_2$, 0.04 M sodium cacodylate trihydrate pH 5.5, 35% (v/v) MPD, 0.002 M hexammine cobalt(III) chloride. Notably, the crystal showed a strong X-ray diffraction to 1.03 Å during data collection. Due to the limited number of published L-nucleic acid crystal structures as a model, we first intended to solve this novel fluoro-modified L-DNA structure by Single-wavelength Anomalous Diffraction (SAD). After soaking the optimal crystals in the iridium(III) hexamine chloride solution, although the strong iridium anomalous signal was observed during data collection and data processing, our attempts to search for Ir^{3+} heavy atoms with high occupancy and build helical model failed.

We then turned to the data collected from the unsoaked crystal and performed molecular replacement. We utilized a published D-DNA structure containing the same sequence (PDB 1d79[23]) and transformed the coordinates into its mirror-image reflection across the *x* axis. Using the created L-DNA as the search model, we successfully obtained the solution and determined the structure (PDB 7KW4) using Phaser in the CCP4 suite.[24] The space group was assigned as hexagonal $P6_522$, with one single strand in an asymmetric unit. After establishing the structure, we re-examined the data from the crystal soaked with Ir^{3+}. We successfully solved the structure by molecular replacement, but could not assign any obvious electron density belonging to Ir^{3+}. It seemed that the observed intense anomalous signal was either from the disordered heavy atoms, which weakly and nonspecifically bound to L-DNA, or from the Ir^{3+} only adhering to the surface of the crystal. The possible reasons for our failure likely include the compact molecular packing inside crystal to inhibit molecular diffusion or the hexamine iridium(III) chloride only binding to weak G:U wobble pair.

As a reflection of the native D-type DNA octamer, our L-DNA duplex adopts a left-handed A-form conformation. The structural features of the L-helical geometry resemble those in the native A-form duplex (Table 2). The base pairs in our L-helical duplex has an average stepwise rise of 3.10 Å, roll angel of 7.12°, slide of −1.13 Å, tilt of 5.22°, and shift of 0.39 Å. The average base pair twist is −33.02°. All the helical parameters are close to those of its native counterpart D-DNA, except for the average twist of base pairs in the opposite direction. All eight L-ribose rings present the C3′-*endo* or C3′-*endo*-2′-*exo* conformations. The entire structure represents the mirror reflection of native D-DNA crystal structure (Figure 1B). We transformed the published structure of D-5′-GTGTACAC-3′ (PDB 1d79) into its mirror reflection and superimposed it with our determined L-8-mer structure. The two structures are highly superimposable, and the r.m.s. deviations between them are 0.088 Å (Figure 1C). The L-DNA duplex contains eight regular Watson−Crick base pairs, including the modified L-type U_F:A pair (Figure 1D). These data indicate that the fluoro-modification does not generate local and overall structural perturbation to the left-handed duplex. Moreover, the high-resolution reveals that the 2′-F-ribose displays the L-type C3′-*endo* pucker conformation (Figure 1E), consistent with the native D-type 2′-F nucleic acid structure.

Table 2. Average Helical Parameters for L- and D-Nucleic Acids 8-mer

	L-5′-GU$_F$GTACAC-3′	D-5′-GTGTACAC-3′ (1d79)
Rise (Å)	3.10	3.17
Roll (deg)	7.12	6.91
Slide (Å)	−1.13	−1.15
Tilt (deg)	5.22	5.46
Shift (Å)	0.39	0.43
Twist (deg)	−33.02	31.98

In summary, we have synthesized the L-type uridine monomer containing 2′-F-modification, as the analogue of L-uridine and mirror reflection of native 2′-F-uridine. Subsequently, we successfully incorporated the residue into L-DNA and L-RNA in quantitative yield. Our systematic thermal study and enzymatic assessment reveal that the fluoro-L-oligonucleotides have notable stability. The CD experiment results validate that the fluoro-modified L-type DNA and RNA adopt the left-handed helical conformations, which present the mirror-image characteristics of their D-type counterparts. Furthermore, our X-ray crystal structure of oligo L-5′-GU$_F$GTACAC-3′ is the first structure of chemically modified L-nucleic acid. The atomic level resolution allows us to examine the structural insights into the modified A-form L-DNA. Indeed, the modified L-DNA presents great structural stability, as evidenced by the overall and local parameters in the L-helix. Although the L-type 2′-F-uridine monomer and its oligonucleotide have been pioneered before,[25] our study here for the first time comprehensively demonstrates its superiority and provides the structural foundation. Therefore, these findings will provide the theoretical framework for the L-nucleic acid therapy design where thermostability is important, including the L-aptamer for disease treatment, L-nanoparticle for drug delivery, and L-molecular beacon for diagnosis.

■ ASSOCIATED CONTENT

Supporting Information

The Supporting Information is available free of charge at https://pubs.acs.org/doi/10.1021/acs.orglett.1c01498.

Experimental procedures, NMR characterization data and LC-MS characterizations for all new compounds, LC-Q-ToF characterizations, melting temperature measurement, serum digestion analysis, circular dichroism measurement and crystallographic statistics for all synthetic oligonucleotides (PDF)

Accession Codes

Atomic coordinates and structure factors for the reported crystal structures have been deposited with the Protein Data bank under accession code 7KW4.

■ AUTHOR INFORMATION

Corresponding Author

Wen Zhang − *Department of Biochemistry and Molecular Biology, Indiana University School of Medicine, Indianapolis, Indiana 46202, United States;* orcid.org/0000-0003-4811-4384; Email: wz15@iu.edu

Authors

Yuliya Dantsu − *Department of Biochemistry and Molecular Biology, Indiana University School of Medicine, Indianapolis, Indiana 46202, United States*

Ying Zhang − *Department of Biochemistry and Molecular Biology, Indiana University School of Medicine, Indianapolis, Indiana 46202, United States*

https://doi.org/10.1021/acs.orglett.1c01498
Org. Lett. 2021, 23, 5007−5011

Complete contact information is available at:
https://pubs.acs.org/10.1021/acs.orglett.1c01498

Notes

The authors declare no competing financial interest.

■ ACKNOWLEDGMENTS

We thank the Zhang lab for helpful discussions, insightful commentary, and careful revision of the manuscript. We thank Dr. L. Zeng and the Chemical Genomics Core at IUSM for LC-MS and NMR analysis. We thank Dr. Zdzislaw Wawrzak from the Life Sciences Collaborative Access Team beamline 21-ID-D at the Advanced Photon Source, Argonne National Laboratory (USA). This research used resources of the Advanced Photon Source, a U.S. Department of Energy (DOE) Office of Science User Facility operated for the DOE Office of Science by Argonne National Laboratory under Contract No. DE-AC02-06CH11357. Use of the LS-CAT Sector 21 was supported by the Michigan Economic Development Corporation and the Michigan Technology Tri-Corridor (Grant 085P1000817).

■ REFERENCES

(1) Wilson, D. S.; Szostak, J. W. In vitro selection of functional nucleic acids. *Annu. Rev. Biochem.* **1999**, *68*, 611−647.
(2) Ellington, A. D.; Szostak, J. W. In vitro selection of RNA molecules that bind specific ligands. *Nature* **1990**, *346*, 818−822.
(3) Zhou, J.; Rossi, J. Aptamers as targeted therapeutics: current potential and challenges. *Nat. Rev. Drug Discovery* **2017**, *16*, 181−202.
(4) Wang, R. E.; Wu, H.; Niu, Y.; Cai, J. Improving the stability of aptamers by chemical modification. *Curr. Med. Chem.* **2011**, *18*, 4126−4138.
(5) Urata, H.; Shinohara, K.; Ogura, E.; Ueda, Y.; Akagi, M. Mirror-image DNA. *J. Am. Chem. Soc.* **1991**, *113*, 8174−8175.
(6) Williams, K. P.; Liu, X.-H.; Schumacher, T. N.; Lin, H. Y.; Ausiello, D. A.; Kim, P. S.; Bartel, D. P. Bioactive and nuclease-resistant L-DNA ligand of vasopressin. *Proc. Natl. Acad. Sci. U. S. A.* **1997**, *94*, 11285−11290.
(7) Dey, S.; Sczepanski, J. T. In vitro selection of l-DNA aptamers that bind a structured d-RNA molecule. *Nucleic Acids Res.* **2020**, *48*, 1669−1680.
(8) Hauser, N. C.; Martinez, R.; Jacob, A.; Rupp, S.; Hoheisel, J. D.; Matysiak, S. Utilising the left-helical conformation of L-DNA for analysing different marker types on a single universal microarray platform. *Nucleic Acids Res.* **2006**, *34*, 5101−5111.
(9) Kabza, A. M.; Sczepanski, J. T. l-DNA-Based Catalytic Hairpin Assembly Circuit. *Molecules* **2020**, *25*, 947.
(10) Damha, M. J.; Giannaris, P. A.; Marfey, P. Antisense L/D-oligodeoxynucleotide chimeras: nuclease stability, base-pairing properties, and activity at directing ribonuclease H. *Biochemistry* **1994**, *33*, 7877−7885.
(11) Lin, C.; Ke, Y.; Li, Z.; Wang, J. H.; Liu, Y.; Yan, H. Mirror image DNA nanostructures for chiral supramolecular assemblies. *Nano Lett.* **2009**, *9*, 433−436.
(12) Gawande, B. N.; Rohloff, J. C.; Carter, J. D.; von Carlowitz, I.; Zhang, C.; Schneider, D. J.; Janjic, N. Selection of DNA aptamers with two modified bases. *Proc. Natl. Acad. Sci. U. S. A.* **2017**, *114*, 2898−2903.
(13) Kabza, A. M.; Sczepanski, J. T. An l-RNA Aptamer with Expanded Chemical Functionality that Inhibits MicroRNA Biogenesis. *ChemBioChem* **2017**, *18*, 1824−1827.
(14) Shi, J.; Du, J.; Ma, T.; Pankiewicz, K. W.; Patterson, S. E.; Tharnish, P. M.; McBrayer, T. R.; Stuyver, L. J.; Otto, M. J.; Chu, C. K. Synthesis and anti-viral activity of a series of d-and l-2′-deoxy-2′-fluororibonucleosides in the subgenomic HCV replicon system. *Bioorg. Med. Chem.* **2005**, *13*, 1641−1652.
(15) Pallan, P. S.; Greene, E. M.; Jicman, P. A.; Pandey, R. K.; Manoharan, M.; Rozners, E.; Egli, M. Unexpected origins of the enhanced pairing affinity of 2′-fluoro-modified RNA. *Nucleic Acids Res.* **2011**, *39*, 3482−3495.
(16) Gesto, D. S.; Cerqueira, N. M. F.S. A.; Fernandes, P. A.; Ramos, M. J. Gemcitabine: a critical nucleoside for cancer therapy. *Curr. Med. Chem.* **2012**, *19*, 1076−1087.
(17) Shi, J.; Du, J.; Ma, T.; Pankiewicz, K.; Patterson, S. E.; Hassan, A. E.; Tharnish, P. M.; McBrayer, T. R.; Lostia, S.; Stuyver, L. J. Synthesis and in vitro Anti-HCV Activity of β-d-and l-2′-Deoxy-2′-Fluororibonucleosides. *Nucleosides, Nucleotides Nucleic Acids* **2005**, *24*, 875−879.
(18) Lewis, M.; Meza-Avina, M. E.; Wei, L.; Crandall, I. E.; Bello, A. M.; Poduch, E.; Liu, Y.; Paige, C. J.; Kain, K. C.; Pai, E. F. Novel interactions of fluorinated nucleotide derivatives targeting orotidine 5′-monophosphate decarboxylase. *J. Med. Chem.* **2011**, *54*, 2891−2901.
(19) Ni, S.; Yao, H.; Wang, L.; Lu, J.; Jiang, F.; Lu, A.; Zhang, G. Chemical modifications of nucleic acid aptamers for therapeutic purposes. *Int. J. Mol. Sci.* **2017**, *18*, 1683.
(20) Hernández, M.; Rodríguez-Lázaro, D.; Esteve, T.; Prat, S.; Pla, M. Development of melting temperature-based SYBR Green I polymerase chain reaction methods for multiplex genetically modified organism detection. *Anal. Biochem.* **2003**, *323*, 164−170.
(21) Wärmländer, S.; Sponer, J. E.; Sponer, J.; Leijon, M. The influence of the thymine C5 methyl group on spontaneous base pair breathing in DNA. *J. Biol. Chem.* **2002**, *277*, 28491−28497.
(22) Patra, A.; Paolillo, M.; Charisse, K.; Manoharan, M.; Rozners, E.; Egli, M. 2′-Fluoro RNA Shows Increased Watson−Crick H-Bonding Strength and Stacking Relative to RNA: Evidence from NMR and Thermodynamic Data. *Angew. Chem.* **2012**, *124*, 12033−12036.
(23) Thota, N.; Li, X.; Bingman, C.; Sundaralingam, M. High-resolution refinement of the hexagonal A-DNA octamer d (GTGTACAC) at 1.4 Å. *Acta Crystallogr., Sect. D: Biol. Crystallogr.* **1993**, *49*, 282−291.
(24) McCoy, A. J.; Grosse-Kunstleve, R. W.; Adams, P. D.; Winn, M. D.; Storoni, L. C.; Read, R. J. Phaser crystallographic software. *J. Appl. Crystallogr.* **2007**, *40*, 658−674.
(25) Bundgaard Jensen, T.; Pasternak, A.; Stahl Madsen, A.; Petersen, M.; Wengel, J. Synthesis and Structural Characterization of 2′-Fluoro-α-L-RNA-Modified Oligonucleotides. *ChemBioChem* **2011**, *12*, 1904−1911.